

Effect of thermal load on the behavior of an adjacent precast, prestressed concrete box-beam bridge that contains ultra-high-performance concrete shear keys with transverse dowels

Ali A. Semendary, Kenneth K. Walsh, Eric P. Steinberg, and Issam Khoury

- Reflective cracks in the overlays due to longitudinal cracks in the shear keys or in the composite decks of adjacent precast, prestressed concrete box-beam bridges have become a critical issue.
- The long-term performance of a bridge with reinforced ultra-high-performance concrete (UHPC) shear keys was investigated for different periods during the first year after its construction.
- No cracks were expected in the shear keys from the field data, and the reinforced UHPC shear keys had enough strength to resist thermal loads, which had the greatest effect on the performance.

Adjacent precast, prestressed concrete box-beam bridges have been in service for many years and have historically performed well. There are many advantages to this type of bridge, including a relatively simple design, ease and speed of construction, and high torsional rigidity.¹⁻⁵ The adjacent box-beam bridge consists of box beams placed side by side and connected with partial- or full-depth shear keys, which are normally grouted using nonshrink grout. Typically, tie rods or transverse post-tensioning, with or without a reinforced concrete deck, are used to enhance the continuity of the bridge in the transverse direction. However, reflective cracks in the overlays or in the composite deck due to the longitudinal cracks in the shear keys have become a critical issue. The main functions of shear keys are to transfer the load and prevent the penetration of water between adjacent beams, which can cause degradation of the shear keys and lead to structural and durability issues. The structural issue is the potential reduction in or loss of load transfer,³ while durability issues could result from salt water penetrating the longitudinal connections, causing corrosion of the beams' reinforcement. Stresses from temperature have been found to be the main cause of longitudinal cracks in shear keys.^{1,3,4,6-9}

The behavior of adjacent precast, prestressed concrete box-beam bridges due to thermal loading was investigated based on field testing of the early-age behavior of a full-scale bridge, field observations of in-service bridges, and finite element modeling. Comprehensive field testing of an in-service bridge under thermal loading over long periods has not yet been performed.

The performance of a full-scale bridge was evaluated for thermal and cyclic loading based on a bridge consisting of four box beams connected by three partial-depth shear keys filled with nonshrink grout.⁶ The results showed cracking at the shear-key interface with the beams for two of the three shear keys when the test was conducted in winter. The cracks totally penetrated the shear key at midspan and partially penetrated another shear key near the abutment. However, when the test was conducted in the summer, cracks were observed at the abutment in all three shear keys three days after casting. In both tests, the cracks from temperature propagated under cyclic loading with no new cracks due to load only. The partial-depth shear keys were also grouted using epoxy, and no cracks were observed under thermal or cyclic loads. However, the difference in thermal expansion between the concrete and the epoxy makes the epoxy undesirable. When the middepth shear keys were grouted using the nonshrink grout, the cracks were reduced because the ungrouted throat assisted the reduction of stresses due to temperature effects.¹

Longitudinal cracks in the shear keys were also identified by inspection in some in-service bridges in Michigan. The results from the field inspections showed that longitudinal cracks at the shear key–beam interface developed due to thermal stresses, especially at early age; through full-depth shear keys; due to high post-tensioning; and when a composite deck had been used.⁴ Finite element modeling was also used to study the temperature effects on the behavior of the adjacent box-beam bridges using either the measured temperature from the field or the design temperature. The results show that temperature was the main cause of the cracks in the shear keys of the adjacent box-beam bridges. However, the finite element model was not verified using actual strain data collected from the bridge.^{7–9}

A significant amount of research has been done to reduce or eliminate shear key cracking by changing the shear key shape or type of grout material.^{10–12} However, the results from these studies were based on small-scale tests or field observations. Because the cracks were observed in the longitudinal joints at the interface between the precast concrete elements and grout materials, transverse forces were applied at discrete locations along the span length using transverse tie rods or post-tensioning strands with or without composite deck.^{2,9,13–15} However, this solution was inadequate to eliminate the reflective cracks in some adjacent box-beam bridges.

Ultra-high-performance concrete (UHPC), along with transverse steel reinforcement, was successfully implemented in the longitudinal connection between two full-scale adjacent box beams. Partial- and full-depth shear keys were grouted

using UHPC and tested under both thermal and cyclic loads. The thermal load was created by pumping steam through the top flanges of the box beams to create temperature gradients, while the cyclic load was applied as concentrated load on each box beam. The results showed that the reinforced UHPC shear key performed well under both thermal and cyclic loading, with no cracks or debonding failure occurring.¹⁶ The testing was conducted in a laboratory environment and involved only two box beams; therefore, field tests to investigate the long-term performance of reinforced UHPC shear key for an in-service bridge under environmental conditions are still needed.

Research significance

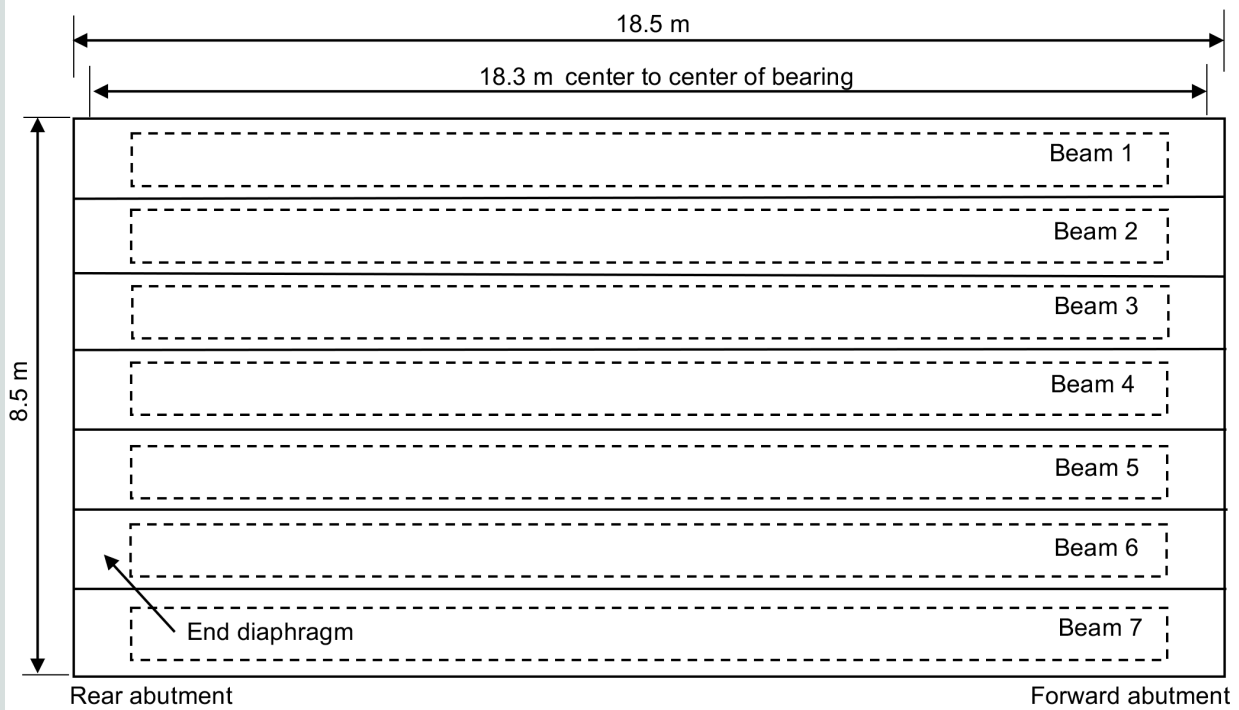
The long-term behavior of adjacent precast, prestressed concrete box-beam bridges with grouted shear keys has not yet been investigated. Furthermore, the behavior of two adjacent box beams with a reinforced UHPC connection under thermal load was studied in a laboratory environment only; therefore, a comprehensive study on adjacent precast, prestressed concrete box-beam bridges using the UHPC shear key connection is still needed. The results from this paper will provide information on the field behavior of the adjacent box-beam bridges with the UHPC connections. These results could also assist in understanding the behavior of the reinforced UHPC shear keys under thermal load.

Bridge description

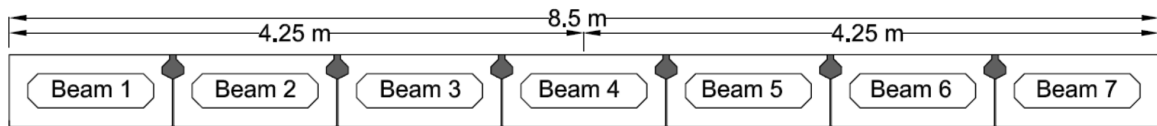
The bridge was constructed on Sollars Road in Fayette County, Ohio, near the town of Washington Court House. Seven adjacent box beams were placed side by side and connected using partial-depth UHPC shear keys with transverse shear reinforcement. The bridge was a 61 ft (19 m) long, 28 ft (8.5 m) wide simple span (**Fig. 1**). The standard Ohio Department of Transportation cross section (B21-48) was used, with the exception of the shear key, which was modified to be consistent with the shear key used in the laboratory tests. The shear key was widened and used transverse steel reinforcement extending from both sides of the beams to create a lap splice staggered at 4 in. (100 mm) spacing (**Fig. 1**). The bridge used 33 in. (840 mm) long diaphragms only at the ends of the box beams. No transverse tie rods, post-tensioning, or composite deck were used in the bridge. The shear keys were covered with plywood before casting with the exception of larger openings at the quarter points along the joints. UHPC—which was prepared using two mixers—was placed in the shear key joints. The mixture consisted of premixture, steel fibers, and liquids. The premixture typically consisted of portland cement, silica fume, ground quartz, and quartz sand. The UHPC included steel fibers at a proportion of 2% by volume. Five days after casting, the plywood forms were removed from the shear keys.

Instrumentation and data collection

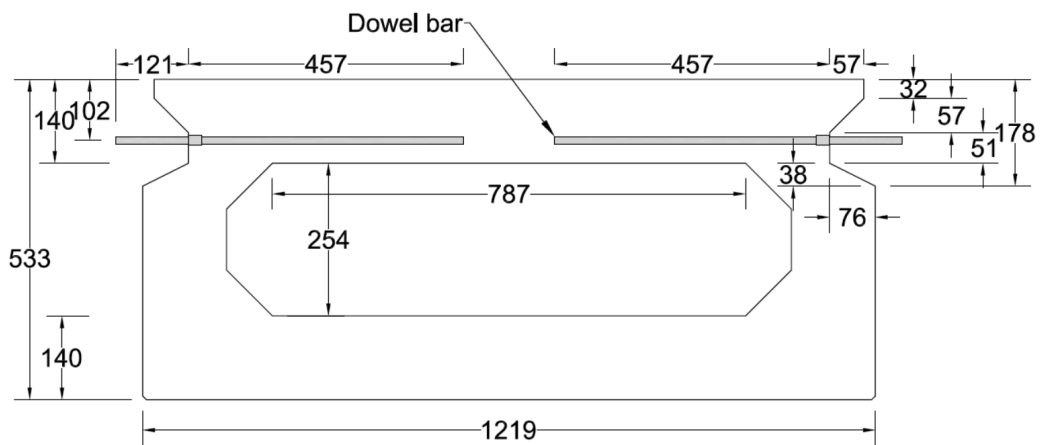
The bridge was instrumented in different locations to investigate its behavior in both hot and cold weather. The first



Top view



Bridge cross section



Beam cross section

Figure 1. Bridge description. Note: Unless otherwise noted, all dimensions are in millimeters. 1 in. = 25.4 mm; 1 ft = 0.305 m.

three beams, numbered 1, 2, and 3 from left to right (Fig. 1), were instrumented using 15 vibrating-wire strain gauges. At midspan, each beam was instrumented with two strain gauges embedded in the top flange in the longitudinal and transverse directions and one gauge embedded in the bottom flange in the longitudinal direction. At the quarter span, each beam was instrumented with two gauges: one embedded in the top flange and the other in the bottom flange in the longitudinal direction only.

Twelve vibrating-wire strain gauges were used to measure the strain in 12 dowel bars. Beams 1, 2, and 3 contained the instrumented dowel bars on the right side of the cross section, while beams 2, 3, and 4 had instrumented dowel bars installed on the left side of the cross section at mid- and quarter spans. For each dowel on the right side of the beam's cross section, one strain gauge was installed on the portion of the dowel that was embedded in the beam. For each dowel on the left side of the beam's cross section, one gauge was installed on the portion of the dowel that was embedded in the key.

The three shear keys between beams 1 and 4 were also instrumented with vibrating-wire strain gauges. Six strain gauges

were installed in the transverse direction at the mid- and quarter spans, while four strain gauges were installed in the longitudinal direction. Shear keys 1 and 3 were instrumented in the longitudinal direction using one strain gauge at the quarter span and one strain gauge at midspan.

Seven KM-100B strain gauges were installed in strain-gauge brackets that had been epoxied to the bottom of the seven beams. The strain gauges were placed in the longitudinal direction at midspan to measure the strain from thermal loading. A steel frame was also installed underneath the bridge at midspan to hold the linear variable differential transformers (LVDTs) during the test. Two strain gauges were also epoxied to a frame in the vertical direction on two columns to measure the strain in the frame from temperature. Three thermocouples were used: one thermocouple on the left column of the frame, one thermocouple on the right column of the frame, and one on the bottom of beam 4. Seven LVDTs were attached to the frame using brackets. The frame was used as a reference surface. Five LVDTs and three thermocouples were added to the instrumentations during the winter period. Joints 4, 5, and 6 were instrumented with three LVDTs at midspan. Two brackets were used to install the LVDTs across the joint in the transverse direction at midspan. Two LVDTs were installed at both ends of beam 7 to monitor the beam movement due to temperature changes. One thermocouple was installed on beam 1 and another on beam 7 to monitor the temperature on both sides of the bridge. One thermocouple was installed on the bottom of beam 3 to monitor the temperature at the bottom. The bridge construction, instrumentation, and testing is discussed in Steinberg et al.¹⁷

Data were collected from August 8 to 16, 2014, after the bridge had been opened to traffic. The data acquisition was zeroed before truck testing, and the environmental monitoring occurred after truck testing was completed. This period was used to investigate the behavior of the bridge due to hot weather. As a result, initial readings may not have been zero at the start of the environmental monitoring. Data were also collected during the period from January 7 to 10, 2015, to monitor the behavior of the bridge during the winter. This was the coldest period during the winter monitoring. The strain data are for the period monitored and do not correspond to the total strain in the member because preexisting strains from self-weight and prestressing are not accounted for in the data. Furthermore, all strain readings were corrected for temperature according to the strain gauge manufacturer's specifications.

Results

Longitudinal behavior of the beams

Figure 2 shows the longitudinal strains and temperatures for the top and bottom flanges at midspan of beam 1 for the monitoring period from August 8 to 16, 2014. The results for beams 2 and 3 at midspan and for all three beams at quarter span were similar and, therefore, are not shown. The top of the beam had larger strains and temperatures compared with the bottom of the beam. The strains in the top flange are inversely related to the temperatures: a decrease in temperature

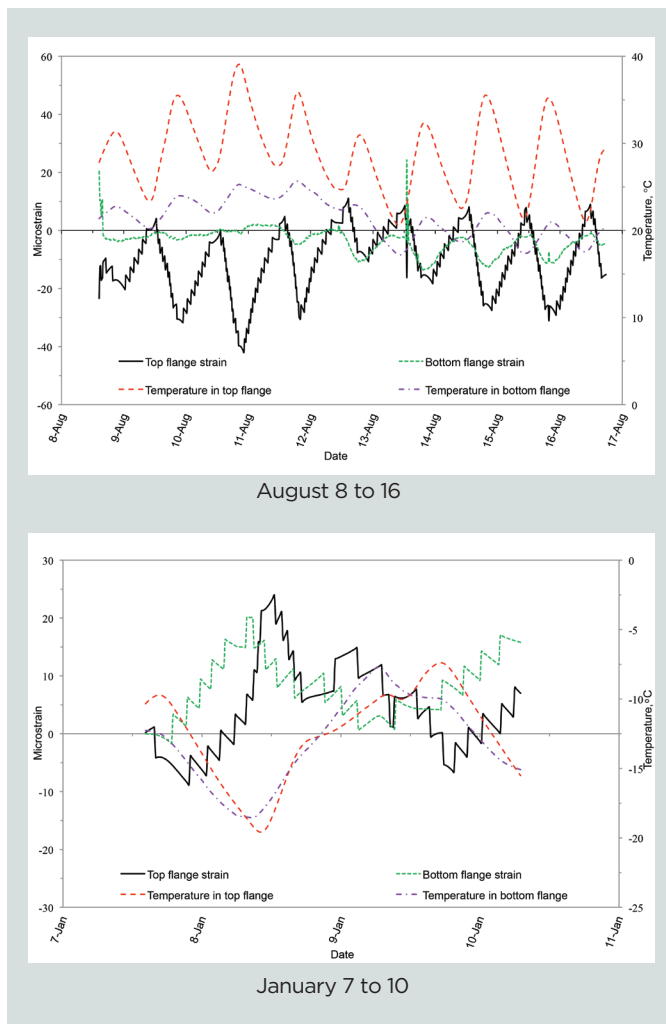


Figure 2. Beam 1 longitudinal strains/temperatures at midspan over time. Note: °F = 1.8(°C) + 32.

caused an increase in strain, and an increase in temperature caused a decrease in strain. The bottom of the beam exhibited a longer time lag between temperature and strain response than the top. The bottom flange strains may also have been influenced by the top flange behavior due to the larger magnitude strains observed on the top. Figure 2 shows that the same spike is present in the strain measurements from all of the other beams on the same day. Although the source of the spike is unknown, it is not believed to be due to temperature effects. The maximum compressive strain in the top flange was about $-42 \mu\epsilon$ (negative strain indicates compression) when the temperature increased to 39°C (100°F).

Figure 2 shows the longitudinal strains and temperatures in the top and bottom flange of beam 1 at midspan from January 7 to 10, 2015. Results obtained at the midspan for beams 2 and 3 and at the quarter span for all three beams were similar and, therefore, are not shown. As expected, the temperature was lower during this period. However, the peak high and low temperatures occurred in the top flange of the beam and there was a delay in the peak temperature for the top compared with the bottom. As previously observed, the strains are inversely related to the temperature: a decrease in temperature caused an increase in strain, and an increase in temperature caused a decrease in strain. There was not a significant delay between the peak temperatures and strains. The maximum tensile strain was about $24 \mu\epsilon$ (positive strain indicates tension) in the top flange when the temperature decreased to -20°C (-4°F).

Longitudinal strain was also measured at the bottom of the beams using exterior strain gauges glued to the bottom surface of each beam for the testing period from August 8 to 16, 2014. The bottom strains were small and the strain increased when the temperature increased, as measured by the internal strain gauges near the bottom. However, the bottom surface strain gauges did not show any time lag between temperature peaks and strain peaks, as measured by the internal strain gauges.

Longitudinal strain was also measured at the bottom surface of the beams using exterior strain gauges mounted to the bottom of each beam for the period from January 7 to 10, 2015. The bottom strains are small and the strain increases when the temperature decreases, as measured by the internal strain gauges near the bottom. However, the bottom surface strain gauges did not show any time lag between temperature peaks and strain peaks compared with the slight time lag for the internal strains.

Figure 3 shows the longitudinal strains measured on the exterior surface of the bottom flanges of beams 1, 2, 3, 5, 6, and 7 in the longitudinal direction at midspan for the period from August 8 to 16, 2014. The results show that the beams generally behaved in the same way. The exception is beam 3, which initially had the opposite behavior of the other beams but eventually showed the same behavior as the other beams. In addition, higher tensile strains were typically in the outer beams and higher compressive strains typically occurred in

the beams toward the interior of the bridge. This is likely due to heating and cooling condition differences between the exterior and interior beams. The maximum bottom compressive strain in the bottom flange was about $-55 \mu\epsilon$ in beam 5 when the temperature increased to 16°C (61°F).

Figure 3 shows the longitudinal strains on the bottom surface of beams 1 through 7 at midspan for the period from January 7 to 10, 2015. The beams had the same general behavior, and the exterior beams (beams 1 and 7) had higher tensile strains. The maximum bottom tensile strain was about $40 \mu\epsilon$ in beam 7 when the temperature decreased to -21°C (-5.8°F).

Longitudinal behavior of the shear keys

Figure 4 provides the measured longitudinal shear key strains and temperatures in shear key 1 at midspan (between beams 1 and 2) for the period from August 8 to 16, 2014. Shear key 1 at quarter span and shear key 3 at mid- and quarter span showed similar behaviors and, therefore, were omitted. The shear key behavior in the longitudinal direction was similar to the beam behavior. As previously observed, the strains are inversely related to the temperatures: a decrease in tempera-

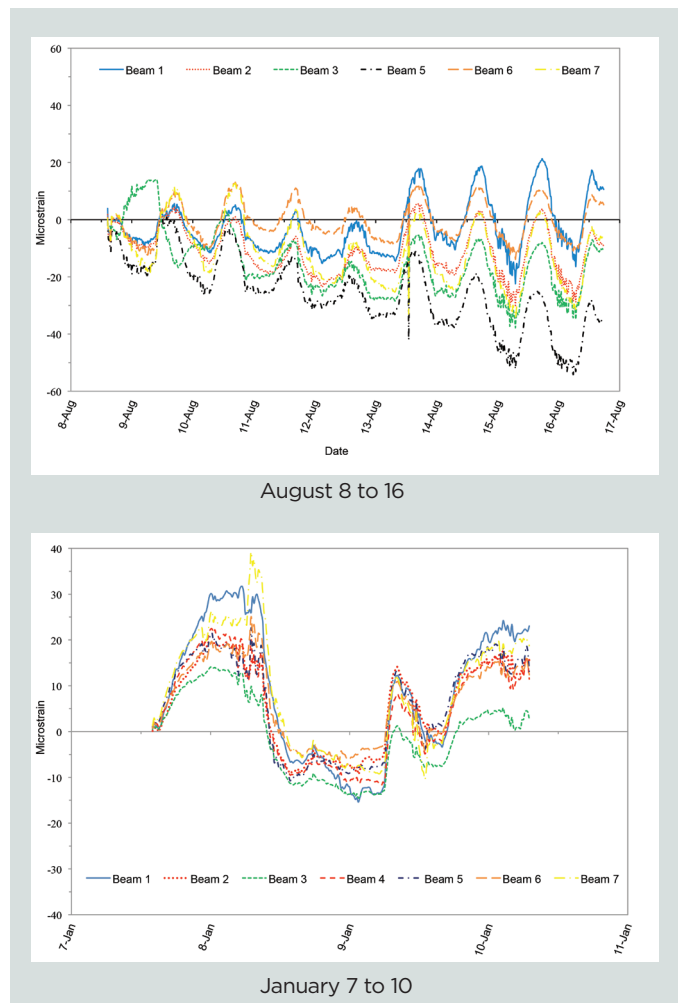
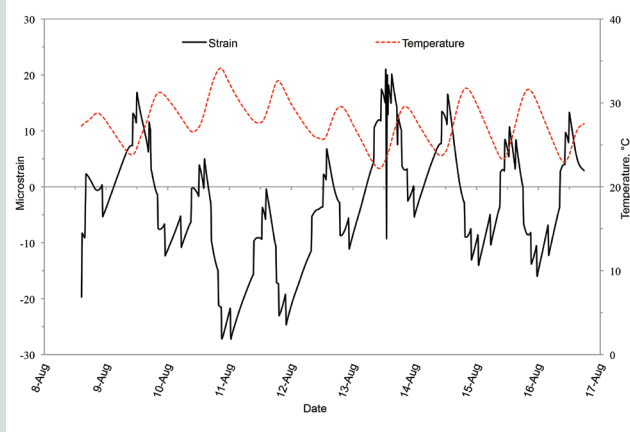
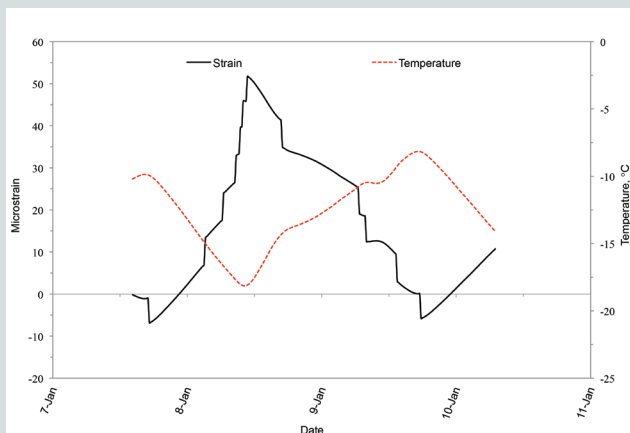


Figure 3. Exterior bottom longitudinal strains at midspan over time.



August 8 to 16



January 7 to 10

Figure 4. Shear key 1 longitudinal strains/temperatures at midspan over time. Note: °F = 1.8(°C) + 32.

ture caused an increase in strain, and an increase in temperature caused a decrease in strain. The maximum compressive strain in the shear key was about $-27 \mu\epsilon$ when the temperature increased to 34°C (93°F).

Figure 4 provides the measured longitudinal shear key strains and temperatures in shear key 1 (between beams 1 and 2) at midspan for the period from January 7 to 10, 2015. Again, the shear key 1 data at the quarter span and the shear key 3 data at mid- and quarter span showed similar behavior and, therefore, were omitted. The shear key behavior in the longitudinal direction was similar to the beam behavior. The strains are inversely related to the temperatures: a decrease in temperature caused an increase in strain, and an increase in temperature caused a decrease in strain. In addition, the recorded tensile strain during this time period was higher than the strains observed in the summer. The maximum measured tensile strain in the shear key was $50 \mu\epsilon$ when the temperature decreased to -18°C (-0.5°F).

Transverse behavior of the beams

As in the longitudinal direction for the period from August 8 to 16, 2014, the transverse strains in beams 1 to 3 are in-

versely related to the temperatures: a decrease in temperature caused an increase in strain, and an increase in temperature caused a decrease in strain. There was also a delay in the strain response from the change in temperatures. The maximum transverse compressive strain in the top flange was about $-23 \mu\epsilon$ when the temperature increased to 34°C (92°F).

The transverse strains in beams 1 through 3 for the period from January 7 to 10, 2015, are also inversely related to the temperatures: a decrease in temperature caused an increase in strain, and an increase in temperature caused a decrease in strain. There was also a delay in the strain response from the change in temperatures. The temperatures were lower during this time period, but the strains showed slightly higher magnitudes compared with the summer data sets. The maximum transverse tensile strain was about $32 \mu\epsilon$ when the temperature decreased to -17°C (1.4°F).

Transverse behavior of the shear keys

Figure 5 shows the transverse strains and temperature in shear key 1 (between beams 1 and 2) at the quarter span for the period from August 8 to 16, 2014. The data for the other shear keys, at the mid- and quarter spans, showed similar behavior but with slightly lower magnitude strain; therefore, this additional data is not provided. Like the longitudinal beam behavior and transverse beam behavior, the strains decreased when the temperature increased and increased when the temperature decreased. The results show that the strains in the shear keys were low due to the small temperature changes. The maximum transverse compressive strain in the shear key was about $-34 \mu\epsilon$ when the temperature increased to 34°C (92°F).

Figure 5 shows the transverse strains and temperatures in shear key 1 (between beams 1 and 2) at the quarter span for the period from January 7 to 10, 2015. The data for the other shear keys at the mid- and quarter spans showed similar behavior but with slightly lower magnitude strain; therefore, these data are not provided. Like the longitudinal beam behavior and transverse beam behavior, the strains decreased when the temperature increased and increased when the temperature decreased. The results show that the strains in the shear keys were low due to the small temperature changes but higher than during the summer periods of monitoring. The maximum transverse tensile strain in the shear key was about $48 \mu\epsilon$ when the temperature decreased to -18°C (-0.4°F).

Dowel bar behavior

The strain of the dowel bars embedded in beams 1 through 3 at midspan increased when the temperature decreased, which is similar to the transverse beam behavior for the period from August 8 to 16, 2014. A slight delay occurred between temperature peaks and the strains. The largest measured compressive strain was about $-24 \mu\epsilon$ and occurred in the dowel bar embedded in beam 1 (not shown) at the quarter span when the temperature increased to 36°C (97°F).

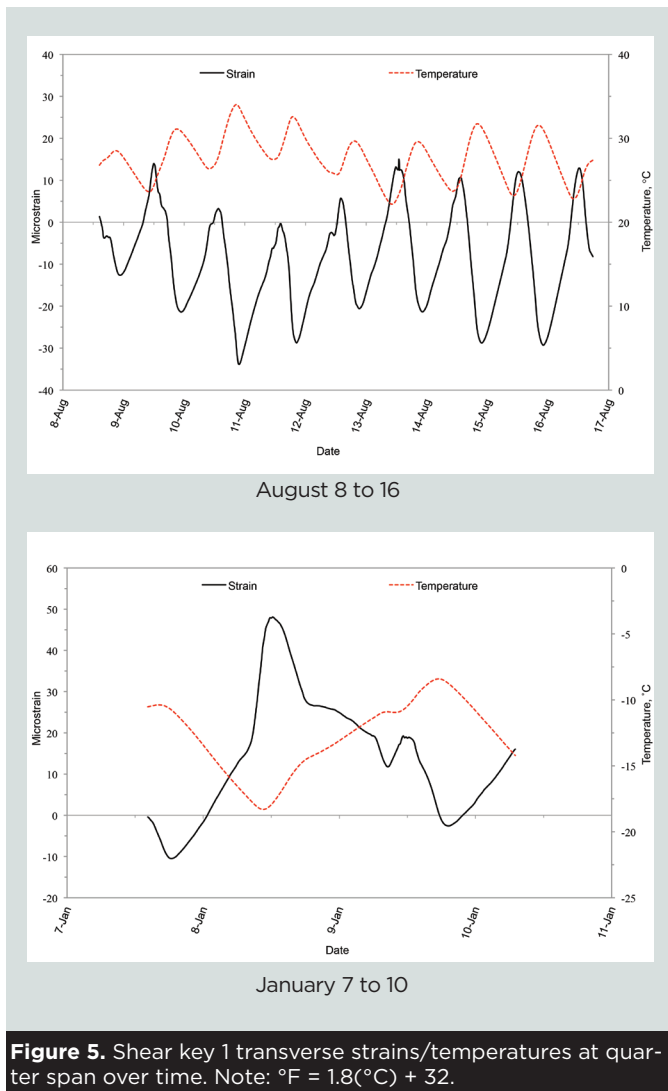


Figure 5. Shear key 1 transverse strains/temperatures at quarter span over time. Note: °F = 1.8(°C) + 32.

The behavior of the dowel bars embedded in beams 1 through 3 at midspan for the period from January 7 to 10, 2015, was the same behavior as for the transverse beams, where the strain increased when the temperature decreased and decreased when the temperature increased. A slight delay occurred between temperature peaks and the strains. The maximum tensile strain in the dowel bar was about 42 $\mu\epsilon$ when the temperature decreased to -19°C (-2.5°F).

Low strains were observed in the dowel bars embedded in shear keys 1 through 3 for the period from August 8 to 16, 2014, and a large time lag was noticed between the strain and temperature peaks. The strain increased when the temperature was increasing, but then the strains began to decrease with further increase in temperature. The largest measured compressive strain was about -12 $\mu\epsilon$ and occurred in the dowel bar embedded in shear key 3 at the quarter span (not shown) when the temperature increased to 24°C (75°F).

The results also showed low strains and a large time lag between the strain and temperature peaks for the dowel bars embedded in shear keys 1 through 3 for the period from January 7 to 10, 2015. The strain decreased when the temperature

was decreasing, but then the strains began to increase with further decrease in temperature. The maximum tensile strain in the dowel bar was about 21 $\mu\epsilon$ and occurred in the dowel bar embedded in shear key 2 at the quarter span (not shown) when the temperature decreased to -17°C (1.4°F).

Deflection, longitudinal movement, and transverse joint movement

Deflection at the bottom of each beam, measured by LVDTs from January 7 to 10, 2015, was investigated. The LVDTs were mounted to a frame that was supported on steel plates and placed beneath the bridge. The data were difficult to interpret because the frame could have moved before data retrieval or the LVDTs could have moved within the brackets holding them to the frame due to a combination of moisture and low temperatures. In addition, the temperature from the top and bottom and throughout the depth of the beam can be different.

Figure 6 shows the midspan deflections and temperatures measured on the bottom surface of beam 7. Downward deflections are positive, and upward deflections are negative. In general, the results show that the beam moved downward when the temperature decreased and upward when the temperature increased. In addition, there was a time lag between the temperature and the bridge deflection. This general trend was also observed in the data for the other beams. However, the data for beam 6 showed little change, which may have been due to the LVDT reaching its limit or not functioning properly. The maximum positive deflection (downward) was 0.108 in. (2.75 mm) when the temperature decreased to -19°C (-2.5°F), while the maximum negative deflection (upward) was 0.2 in. (5 mm) when the temperature increased to -9°C (16°F). Overall the deflections were small.

Figure 7 shows the longitudinal movements at the ends of beam 7 relative to the abutments. The ends of each beam contain 2 in. (50 mm) diameter holes with a 1 in. (25 mm) diameter dowel. The dowels were the height of the beams plus

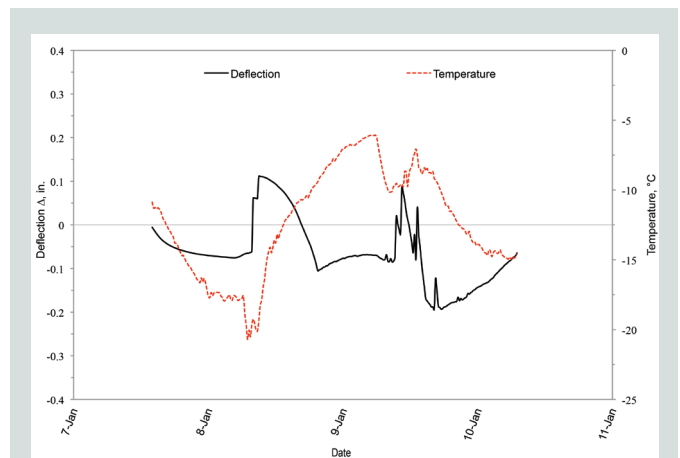


Figure 6. Deflections and bottom surface temperatures over time for beam 7 at midspan. Note: 1 in. = 25.4 mm; °F = 1.8(°C) + 32.

12 in. (265 mm) into the abutments. The dowels at the rear abutment were grouted to create a fixed-support condition. The dowel holes at the forward abutment were filled with joint sealer to create an expansion-joint support condition. The results show that when the temperature decreased, both ends had approximately the same small movements. A positive movement in the figures means that the beam expanded, and a negative movement means it contracted. The beam expanded when the temperature increased and contracted when temperature decreased. The beam end at the forward abutment (right) had slightly more movement due to the joint sealer used in the grouting of the dowel hole.

The joint movement in the transverse direction at the bottom of joints 4, 5, and 6 were measured using LVDTs. Unfortunately, the LVDT readings on joint 6 were unreliable and were, therefore, omitted. However, the data from joints 4 and 5 were similar and consistent (Fig. 8). In addition, the LVDTs were mounted directly onto the beams, so the data were easier to interpret. Small movements were observed, but the trend shows that the joint closed when the temperature decreased and opened when the temperature increased. There was also a delay in the joint movement response compared with the

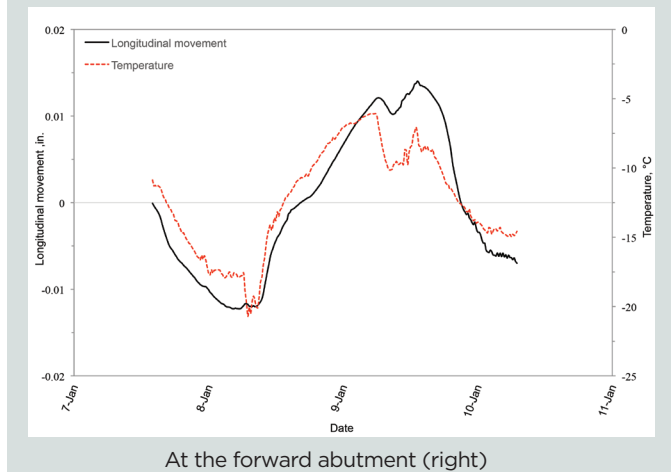
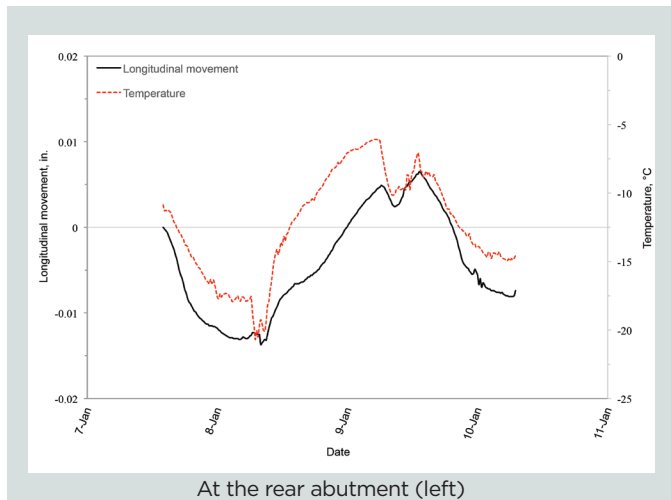


Figure 7. Beam 7 longitudinal movement and bottom surface temperatures over time. Note: 1 in. = 25.4 mm; °F = 1.8(°C) + 32.

temperature readings. The joint movement may be related to the higher coefficient of thermal expansion of the UHPC compared with that of the concrete used in the beams. The joint closing may be related to the higher contraction of the UHPC compared with the concrete due to the higher coefficient of thermal expansion or to the high resistance to this contraction at the interface when the temperature decreases or increases.

Discussion

Comparison between thermal and static truck load behaviors

The maximum longitudinal tensile strain at the exterior bottom of beam 7 at midspan was about $40 \mu\epsilon$ during the winter period. However, the maximum exterior bottom tensile strain was $109 \mu\epsilon$ on beam 7 when the bridge was loaded with two trucks at midspan with a total weight of 109.5 kip (487.1 kN). The results showed that the tensile strain from loading was twice as large as the value from temperature.

The maximum positive deflection (downward) was 0.11 in. (2.8 mm) and the maximum negative deflection (upward) was 0.2 in. (5 mm) from temperature. However, the maximum deflection of the bridge due to the static truck load was found to be on beam 7 and was 0.48 in. (12 mm) when the bridge was loaded with two trucks at midspan with a total weight of 109.5 kip (487.1 kN).¹⁸ The deflection from the temperature was lower than the deflection from the static truck load.

The highest tensile strains from all strain gauges were observed when the temperature decreased. This means that the bridge components exhibited high tensile strains when the temperature difference between top and bottom was negative. The negative temperature difference could be created if the top was colder than the bottom and can be observed in both cold and hot weather. For the data collected in January, the temperature difference was higher than the temperature difference measured in August. The maximum transverse tensile strain in

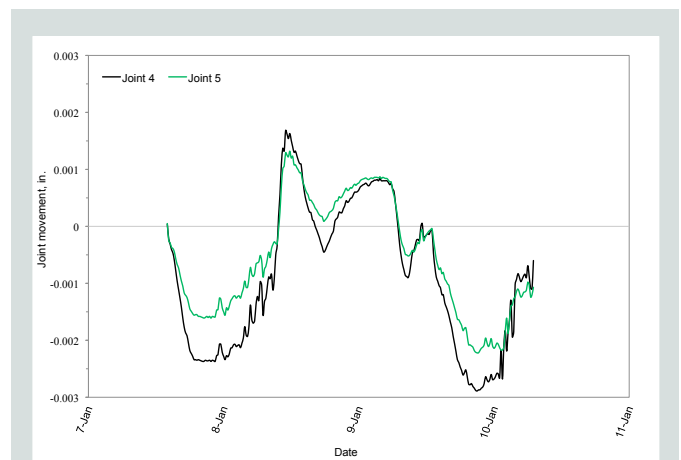


Figure 8. Joint movement across joints 4 and 5 over time. Note: 1 in. = 25.4 mm.

Table 1. Longitudinal strain in the top and bottom flange of beams 1 through 3 at mid- and quarter span due to temperature and static truck load

Type of load	Location	Strain gauge location	Strain, $\mu\epsilon$		
			Beam 1	Beam 2	Beam 3
Temperature load at 12:00 p.m. on January 8	Midspan	Top	23	23	22
		Bottom	12	7	7
	Quarter span	Top	22	26	n.d.
		Bottom	16	n.d.	n.d.
Two trucks back to back on left lane	Midspan	Top	-79*	-53*	-64*
		Bottom	77	73	53
	Quarter span	Top	-52*	-31*	n.d.
		Bottom	49	n.d.	n.d.

Note: n.d. = no data because the gauges were disconnected due to data acquisition capacity.
*Negative strain indicates compression.

the shear keys was observed on January 8 at 12:00 p.m. Therefore, the data from this specific period will be discussed.

The longitudinal interior strains in the top and bottom flanges of beams 1 through 3 due to the temperature from this period were compared with the longitudinal interior strains due to the static truck load at mid- and quarter spans (**Table 1**). The results from the temperature show that the beam exhibited tensile strain when the temperature decreased in both the top and bottom flanges. However, the results from the static truck load, when the bridge was loaded with two trucks back to back with a total weight of 109.5 kip (487.1 kN), show that the top flange exhibited compressive strain while the bottom flange exhibited tensile strain at both mid- and quarter spans. The strain in the bottom flange due to static truck load was higher than the values due to temperature. The strains due to truck load exclude temperature effects.

The longitudinal strains due to temperature were compared with the longitudinal strains due to static truck load in shear keys 1 and 3 (**Table 2**). The maximum compressive strain was observed when the bridge was loaded with two trucks back to back.¹⁹ The results show that the shear keys exhibited compressive strain due to static truck load. However, tensile strain due to temperature load was observed in the shear key. A comparison of the results from Table 1 with the result from Table 2 shows that the longitudinal tensile strains in the shear keys due to temperature load were higher than the longitudinal tensile strain in the top flange of the beams, though the temperature was the same.

The transverse strain due to temperature in the top flange of beams 1 through 3 at midspan was compared with the strain due to static truck load (**Table 3**). The maximum transverse tensile strain was observed when the bridge was loaded with two trucks at midspan with total weight of 109.5 kip

Table 2. Longitudinal strain in shear keys 1 and 3 at mid- and quarter span due to temperature and static truck load

Type of load	Location	Strain, $\mu\epsilon$	
		Shear key 1	Shear key 3
Temperature load at 12:00 p.m. on January 8	Midspan	50	46
	Quarter span	50	39
Two trucks back to back on left lane	Midspan	-64*	-65*
	Quarter span	-35*	-46*

* Negative strain indicates compression.

Table 3. Transverse strain in the top flange of beams 1 through 3 at midspan due to temperature and static truck load

Type of load	Strain, $\mu\epsilon$		
	Beam 1	Beam 2	Beam 3
Temperature load at 12:00 p.m. on January 8	31	27	31
Two trucks at midspan	28	12	11

(487.1 kN). The results show that the bridge exhibited tensile strain at the top of each beam in the transverse direction. The transverse tensile strain from temperature was slightly higher than the strain from static truck load.

The transverse strain due to temperature in shear keys 1 through 3 at mid- and quarter span was compared with the

Table 4. Transverse strain in the shear keys 1 through 3 at mid- and quarter span due to temperature and static truck load

Type of load	Location	Strain, $\mu\epsilon$		
		Shear key 1	Shear key 2	Shear key 3
Temperature load at 12:00 p.m. on January 8	Midspan	17	31	19
	Quarter span	48	30	17
Two trucks back to back on left lane	Midspan	10	6	11
	Quarter span	7	4	13

Table 5. Strain in the dowel bar embedded in right side of the cross section of beams 1 through 3 at mid- and quarter span due to temperature and static truck load

Type of load	Location	Strain, $\mu\epsilon$		
		Dowel bar 1	Dowel bar 2	Dowel bar 3
Temperature load at 12:00 p.m. on January 8	Midspan	29	36	40
	Quarter span	26	n/a	n/a
Two trucks back to back on left lane	Midspan	23	20	13
	Quarter span	18	n/a	n/a

Note: n/a = not applicable because the gauges were disconnected due to data acquisition capacity.

Table 6. Strain in the dowel bar embedded shear keys 1 through 3 at mid- and quarter span due to temperature and static truck load

Type of load	Location	Strain, $\mu\epsilon$		
		Dowel bar 1	Dowel bar 2	Dowel bar 3
Temperature load at 12:00 p.m. on January 8	Midspan	5	9	3
	Quarter span	3	21	3
Two trucks back to back on left lane	Midspan	9	8	15
	Quarter span	7	3	12

strain due to static truck load (**Table 4**). The maximum transverse tensile strain was observed when the bridge was loaded with two trucks back to back with a total weight of 109.5 kip (487.1 kN).¹⁹ The results show that the shear keys exhibited tensile strain from both the temperature and static truck load in the transverse direction. The transverse tensile strains from temperature were higher than the strains from static truck load.

The axial strains due to temperature in the dowel bar for the part embedded in the beam and the part embedded in the shear keys at mid- and quarter spans were compared with the axial strains due to static truck load (**Tables 5 and 6**). The maximum axial strain from the truck load was observed when the bridge was loaded with two trucks back to back with a total weight of 109.5 kip (487.1 kN).¹⁹ The results show that the dowel exhibited tensile strain from both the temperature and static truck load. The axial tensile strains from tempera-

ture were higher than the strains from static truck load for the part embedded in the beams and slightly higher for the part embedded in the shear keys. The temperature had more influence on the transverse behavior relative to static load than on the longitudinal behavior. It also had more influence away from the support.

Comparison of the measured strains with the allowable limits

The main objective of shear keys is to transfer the load between adjacent beams in the transverse direction. To obtain adequate load transfer, shear key tensile strength, interface bond strength, and beam transverse tensile strength should be sufficient to resist the applied load that develops due to truck or thermal loads. The preexisting strains due to self-weight, prestressing, and previous environmental effects, cannot be

accounted for in a comparison because the gauges were not continuously monitored over the entire project history. The compressive strength of the concrete used in the box beams was 11 ksi (76 MPa), while the compressive strength of the UHPC was 22.0 ksi (152 MPa); both strengths were determined from cylinder tests. The modulus of elasticity of the box beam was calculated using the typical equation from ACI's *Building Code Requirements for Structural Concrete (ACI 318-14) and Commentary (ACI 318R-14)*²⁰ and found to be 5987.8 ksi (41,286 MPa). For UHPC, the modulus of elasticity was calculated using the equation from Russell and Graybeal²¹ and found to be 7267.7 ksi (50,111 MPa). The modulus of elasticity of the steel was assumed to be 29,000 ksi (200,000 MPa).

The maximum transverse tensile strain at the center of the top flange was 31 $\mu\epsilon$ in beam 1, which is equivalent to 0.186 ksi (1.28 MPa). The maximum transverse tensile strain in the UHPC was 48 $\mu\epsilon$ in shear key 1 at the quarter span, which is equivalent to 0.35 ksi (2.4 MPa). The maximum tensile strain in the dowel bar was 40 $\mu\epsilon$, which is equivalent to 1.2 ksi (8.3 MPa). The allowable tensile strength for the precast concrete beam was found to be 0.788 ksi (5.43 MPa) using the typical equation from ACI 318-14. The allowable tensile strength of UHPC was found to be 0.989 ksi (6.82 MPa).¹⁹ The interface bond strength between the precast concrete and UHPC at the exposed aggregate surface under a pull-off bond test at 14 days was found to be 0.553 ksi (3.81 MPa).²² The steel tensile strength was assumed to be 60 ksi (414 MPa).

The results show that the applied stresses due to temperature and truck load caused no failure in the transverse direction of the precast concrete beams, in the UHPC shear keys, at the interface between the two materials, or in the steel. The results show that the new shear key configuration had adequate capacity to resist both static and thermal loads.

Conclusion

The long-term behavior of the first adjacent precast, prestressed concrete box-beam bridge in the United States using reinforced UHPC shear keys was investigated under thermal load. The data from the environmental monitoring can only account for the behavior during the period being examined. Any preexisting strains, such as self-weight, prestressing, and previous environmental effects, cannot be accounted for because the strain gauges were not continuously monitored over the entire project history. However, the environmental monitoring still provided the following valuable results.

- August 8 to 16, 2014

- The results show that both tension and compression strains were inversely related to the temperature changes for the top. As the top of the beam increased in temperature, it attempted to expand. The expansion was restrained and generated compressive strains. The opposite occurred as the beam cooled. The bottom of

the beams exhibited small longitudinal strains from the temperature changes that were also smaller compared with the top.

- Higher tensile strains measured by bottom surface gauges were typically observed in the outer beams, and higher compressive strains were typically observed in the beams toward the interior of the bridge. This was likely due to heating and cooling condition differences.
- The longitudinal strains in the shear key showed the same behavior as the top longitudinal behavior of the beam, which emphasized that high bond strength existed at the interface.
- The top transverse beam behavior was the same as the top longitudinal beam behavior, though there was a slight delay from temperature peaks to strain peaks.
- The transverse strains in the shear key were small compared with transverse strain data from January.
- The strains for the dowel bars embedded in the shear keys show a longer delay between the temperature peaks and strain peaks.
- January 7 to 10, 2015
 - As expected, the temperatures were lower during this period. However, the peak high and low temperatures occurred in the top flange of the beam and there was a delay in the peak temperatures for the top compared with the bottom.
 - In general, based on the data, the behavior of the bridge was the same as during the August data period, other than the magnitude. The transverse results show higher tensile strains, as expected from the colder temperatures.
 - The transverse strains in the shear key and the axial strain in the dowel bars were higher than the strains shown in the August data.
 - The movements of the girders monitored during this period were small, and there was typically a delay between peak temperatures and peak movements. The beams moved downward with a decrease in temperature and upward with an increase in temperature.
 - The monitored beam expanded longitudinally during increasing temperatures and contracted during decreasing temperatures. For the joints monitored, the joints closed with a decrease in temperature and opened with an increase in temperature.
- The temperature had a greater effect on the behavior of the shear key than the static truck load. Furthermore, a

tensile strain was observed in the transverse direction from both static and thermal loads.

- No cracks were expected in the shear keys or in the beam because the measured strains, which were converted to stresses, were lower than the allowable tensile strengths.
- The strain from the temperature was unable to cause any type of failure in the box beam, UHPC, dowel bar, or at the interface.
- A minimum interface bond strength of 0.35 ksi (2.4 MPa) under temperature load based on the data analysis might be recommended to prevent interface bond failure when selecting grout material for adjacent box-beam bridges.

The authors recommend that shear keys be cast with UHPC at relatively lower temperatures so that any subsequent temperature change is likely to cause a temperature increase, thereby generating compressive strain at the joints.

Acknowledgments

The research team would like to extend its gratitude to Steve Luebbe, the Fayette County Engineer; Tim Keller of the Office of Structural Engineering at the Ohio Department of Transportation; Benjamin Graybeal of the Turner-Fairbank Highway Research Center, Federal Highway Administration; Luke Dlugosz and Kyle Nachuk of LaFarge North America; Vic Perry of V.iConsult Inc. (formerly of LaFarge North America); Robert Ballard and Rob Cunningham from URS; and the bridge general contractor, The Righter Company Inc. in Columbus, Ohio.

References

1. Miller, R. A., G. M. Hlavacs, T. Long, and A. Greuel. 1999. "Full-Scale Testing of Shear Keys for Adjacent Box Girder Bridges." *PCI Journal* 44 (6): 80–90.
2. El-Remaily, A., M. K. Tadros, T. Yamane, and G. Krause. 1996. "Transverse Design of Adjacent Precast Prestressed Concrete Box Girder Bridges." *PCI Journal* 41 (4): 96–113.
3. Russell, H. G. 2009. *Adjacent Precast Concrete Box Beam Bridges: Connection Details*. NCHRP (National Cooperative Highway Research Program) synthesis report 393. Washington, DC: Transportation Research Board.
4. Attanayake, U., and H. Aktan. 2015. "First-Generation ABC System, Evolving Design, and Half a Century of Performance: Michigan Side-by-Side Box-Beam Bridges." *Journal of Performance of Constructed Facilities* 29 (3). <https://ascelibrary.org/doi/abs/10.1061/%28ASCE%29CF.1943-5509.0000526>.
5. Steinberg, E. P., and A. A. Semendary. 2016. "Evaluation of Transverse Tie Rods in a 50-Year-Old Adjacent Prestressed Concrete Box Beam Bridge." *Journal of Bridge Engineering* 22 (3). <https://ascelibrary.org/doi/abs/10.1061/%28ASCE%29BE.1943-5592.0001001>.
6. Hlavacs, G. M., T. Long, R. A. Miller, and T. M. Baseheart. 1997. "Nondestructive Determination of Response of Shear Keys to Environmental and Structural Cyclic Loading." *Transportation Research Record* 1574: 18–24.
7. Dong, X. 2002. "Traffic Forces and Temperature Effects on Shear Key Connections for Adjacent Box Girder Bridge." PhD diss. University of Cincinnati, Cincinnati, OH.
8. Ulku, E., U. Attanayake, and H. Aktan. 2010. "Rationally Designed Staged Posttension Abates Reflective Cracking on Side by Side Box Beam Bridge Deck." In *Transportation Research Board (TRB) 89th Annual Meeting: Compendium of Papers, January 10–14, 2010*. Washington, DC: Transportation Research Board.
9. Grace, N. F., E. A. Jensen, and M. R. Bebawy. 2012. "Transverse Post-tensioning Arrangement for Side-by-Side Box-Beam Bridges." *PCI Journal* 57 (2): 48–63.
10. Gulyas, R. J., G. J. Wirthlin, and J. T. Champa. 1995. "Evaluation of Keyway Grout Test Methods for Precast Concrete Bridges." *PCI Journal* 40 (1): 44–57.
11. Lall, J., S. Alampalli, and E. F. DiCocco. 1998. "Performance of Full-Depth Shear Keys in Adjacent Prestressed Box Beam Bridges." *PCI Journal* 43 (2): 72–79.
12. Issa, M. A., C. L. Ribeiro do Valle, H. A. Abdalla, S. Islam, and M. A. Issa. 2003. "Performance of Transverse Joint Grout Materials in Full-Depth Precast Concrete Bridge Deck Systems." *PCI Journal* 48 (4): 92–103.
13. Hanna, K. E., G. Morcou, and M. K. Tadros. 2009. "Transverse Post-tensioning Design and Detailing of Precast Prestressed Concrete Adjacent Box-Girder Bridges." *PCI Journal* 54 (4): 160–174.
14. Fu, C. C., Z. Pan, and M. S. Ahmed. 2011. "Transverse Post-tensioning Design of Adjacent Precast Solid Multi-beam Bridges." *Journal of Performance of Constructed Facilities* 25 (3): 223–230.
15. Hansen, J., K. Hanna, and M. K. Tadros. 2012. "Simplified Transverse Post-tensioning Construction and Maintenance of Adjacent Box Girders." *PCI Journal* 57 (2): 64–79.
16. Yuan, J., and B. Graybeal. 2016. "Full-Scale Testing of Shear Key Details for Precast Concrete Box-Beam Bridges." *Journal of Bridge Engineering* 21 (9). <https://ascelibrary.org/doi/abs/10.1061/%28ASCE%29BE.1943-5592.0000906>.

17. Steinberg, E., A. Semendary, and K. Walsh. 2015. "Adjacent Precast Box Beam Bridges Using UHPC Longitudinal Joints." *The Construction Specifier* 68 (8): 28–42.
18. Steinberg, E., A. Semendary, and K. Walsh. 2016. "Static Load Truck Testing of an Adjacent Box Beam Bridge Containing Ultra High Performance Concrete (UHPC) Longitudinal Joints." In *The PCI National Bridge Conference: Proceedings, March 3–6, 2016, Nashville, Tennessee*. Chicago, IL: PCI.
19. Steinberg, E., A. Semendary, and K. Walsh. 2016. "Implementing Ultra High Performance Concrete (UHPC) with Dowel Bars in Longitudinal Joints (Shear Key) in an Adjacent Box Beam Bridge." In *First International Interactive Symposium on UHPC: Proceedings, July 18–20, 2016, Des Moines, Iowa*. Ames, IA: Iowa State University.
20. ACI (American Concrete Institute) Committee 318. 2014. *Building Code Requirements for Structural Concrete (ACI 318-14) and Commentary (ACI 318R-14)*. Farmington Hills, MI: ACI.
21. Russell, H., and B. Graybeal. 2013. "Ultra-high Performance Concrete: A State-of-the-Art Report for the Bridge Community." FHWA-HRT-13-060. McLean, VA: Office of Infrastructure Research & Development, Federal Highway Administration.
22. De la Varga, I., Z. Haber, and B. Graybeal. 2016. "Performance of Grouted Connections for Prefabricated Bridge Elements—Part I: Material-Level Investigation on Shrinkage and Bond." In *The PCI National Bridge Conference: Proceedings, March 3–6, 2016, Nashville, Tennessee*. Chicago, IL: PCI.

About the authors



Ali A. Semendary is a PhD candidate in the Department of Civil Engineering at Ohio University in Athens, Ohio.



Kenneth K. Walsh, PhD, is an associate professor in the Department of Civil Engineering at Ohio University.



Eric P. Steinberg, PhD, PE, is a professor in the Department of Civil Engineering at Ohio University.



Issam Khoury, PhD, PE, is an assistant professor in the Department of Civil Engineering at Ohio University.

Abstract

Adjacent precast, prestressed concrete box-beam bridges have been in service and have performed well for many years. However, reflective cracks in the overlays or in the composite deck due to longitudinal cracks in the shear keys have become a critical issue. These cracks were believed to develop due to thermal load and propagate due to live load or through a combination of the two. Little research has been done to study the early-age behavior of these bridges due to thermal loading, and none has been conducted to investigate the behavior of these bridges in the long term. The behavior of the first adjacent box-beam bridge in the United States containing ultra-high-performance concrete (UHPC) shear keys with transverse dowels was investigated under thermal load. Unfortunately, little to no research has been done to investigate the long-term behavior of field-cast UHPC connections. In this paper, the long-term performance of a bridge with reinforced UHPC shear keys was investigated for different periods during the first year after its construction. The results due to thermal loads were compared with the results from static truck loads. No cracks were expected in the shear keys from the field data. Furthermore, the reinforced UHPC shear keys had enough strength to resist thermal loads, which had the greatest effect on the performance.

Keywords

Box beam, dowel bar, longitudinal crack, shear key, temperature, thermal load, ultra-high-performance concrete.

Review policy

This paper was reviewed in accordance with the Precast/Prestressed Concrete Institute's peer-review process.

Reader comments

Please address any reader comments to *PCI Journal* editor-in-chief Emily Lorenz at elorenz@pci.org or Precast/Prestressed Concrete Institute, c/o *PCI Journal*, 200 W. Adams St., Suite 2100, Chicago, IL 60606.